Femtosecond time-resolved spectroscopy of self-trapping processes of holes and electron-hole pairs in alkali bromide crystals

T. Sugiyama, H. Fujiwara, T. Suzuki, and K. Tanimura
Department of Physics, Nagoya University, Furo-cho, Chikusa, Nagoya 464-01, Japan
(Received 22 March 1996; revised manuscript received 12 August 1996)

The dynamics of the lattice relaxation of holes and electron-hole (e-h) pairs generated by the band-gap excitation in alkali bromide crystals has been studied in femtosecond time regime at temperature range from 6 to 300 K. In KBr including electron-trapping impurities, where relaxation of holes takes place without interaction with electrons, it is found that the self-trapped hole in the form of a halogen-molecular ion, the V_K center, is generated via a transient localized-hole center as a precursor. This transient hole center shows broad optical absorption bands in the visible region and has a lifetime of about 3 ps at 273 K. It is found that in pure KBr and RbBr, the relaxation processes of (e-h) pairs have two distinct stages. In the first stage, which terminates within 6 ps after excitation, the transient hole centers are generated as in doped specimens, and their interaction with electrons results in the fast formation of a Frenkel pair consisting of an F center, a halogen vacancy trapping an electron, and an H center, an interstitial halogen atom. Also, an intermediate state is formed in the first stage, and the state is ascribed to the self-trapped exciton (STE) with the on-center configuration on the basis of its spectroscopic features. The second stage of the relaxation, which lasts over 100 ps at low temperatures, comprises the off-center relaxation of the on-center STE formed in the first stage into Frenkel pairs and STE's with the off-center configuration. Relaxation pathways and characteristics including temperature dependence are discussed based on the experimental results and their analysis in terms of a rate-equation model. [S0163-1829(96)01545-7]

I. INTRODUCTION

In many solids with strong electron-phonon coupling, drastic lattice-structure modifications are induced by the electronic excitation. These include Frenkel-pair production in metal halides,[1–5] atomic desorption from solid surfaces,[6] structural changes in amorphous solids,[7] and phase transformation in low-dimensional solids.[8] Based on the results of extensive studies on these phenomena, it has been proposed that the interaction between or among photogenerated excited species during their relaxation plays an important role in the structural changes.[1,9–11] In order to examine the validity of the models proposed and to understand the mechanisms of these phenomena from a more microscopic view point, it is essential to trace the dynamics of the interaction of excited species during relaxation on the time scale of lattice vibrations. In this paper, we study the dynamics of the lattice relaxation of photogenerated electron-hole (e-h) pairs which leads to the formation of lattice defects of Frenkel type in alkali bromide crystals by means of femtosecond time-resolved spectroscopy.

In alkali halides, the lattice relaxation of holes, excitons and free (e-h) pairs have been studied extensively, and self-trapping of holes and of excitons has been well documented.[2] The self-trapped hole (STH) in all alkali halides is known to have only one stable configuration in the form of an X_2^- molecular ion (X denotes a halogen atom) occupying two neighboring halogen-lattice sites, known as the V_K center.[12] In contrast, experimentally observed spectroscopic properties of relaxed configurations of excitons can be understood only assuming the existence of several different configurations.[2,13–15] These include three configurations of the self-trapped excitons (STE's) responsible for the intrinsic luminescence bands, which are often classified as types I, II, and III, and the Frenkel pair consisting of an F center, a halogen vacancy trapping an electron, and an H center, an interstitial halogen atom in the form of X_2^- molecular ion occupying a single halogen-lattice site. The Frenkel pair is called hereafter the F-H pair.

Recent studies of resonance Raman spectroscopy,[16,17] together with spectroscopic features of optical absorption[14,18] and luminescence[13] related to STE's have shown clearly that the type-I STE is essentially a V_K center which has trapped an electron. Since the hole component of the STE in this configuration maintains almost the same vibrational and electronic properties as those of the V_K center, this type-I STE is usually referred to as the on-center STE.[2,19] On the other hand, the type-III STE is essentially a nearest-neighbor pair of an F center and an H center.[17] Since the X_2^- molecular ion is displaced significantly from the V_K-center position along a $\langle 110 \rangle$ direction, this configuration is referred to as the off-center STE.[2] The type-II STE is presumed to have a configuration intermediate between the two. In Fig. 1, the structures of the on- and off-center STE's are shown schematically, together with that of the F-H pair. Evidently, the difference in these configurations is attributed primarily to the location of the X_2^- molecular ion with respect to the position of the trapped electron; the F-H pair is that in which the X_2^- molecular ion is displaced over at least a few lattice distance.[20] In most crystals, two or more of these configurations can coexist, and the presence of these different relaxed configurations of excitons is regarded as a manifestation of the strong interplay between the electron-phonon and hole-phonon interactions.[1]

Although the properties of STE's and of F-H pairs have

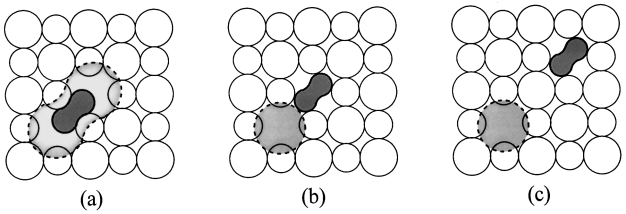

FIG. 1. Schematic diagram of the on-center self-trapped exciton (a), the off-center self-trapped exciton (b) and an F-H pair (c) in alkali halides. Small and large circles show alkali and halogen ions, respectively.

been studied in detail, the dynamics of the lattice relaxation leading to these different configurations is not yet known. Time-resolved spectroscopic studies of the relaxation of $(e$-$h)$ pairs in picosecond and more longer time regimes[21,22] were not able to follow the primary steps of the relaxation, leaving several fundamental questions unsolved. In particular, the mechanism of the Frenkel-pair generation has not yet been determined unambiguously, although many models have been proposed.[4,23–28] Recent femtosecond time-resolved spectroscopic studies have shown that this method is certainly able to reveal the primary steps of lattice relaxation,[29–31] and here we use this technique to study this aspect of the relaxation of $(e$-$h)$ pairs in alkali bromides of KBr and RbBr. Both of the crystals are typical examples of the alkali halide crystals in which all of the three configurations shown in Fig. 1 are formed with high efficiencies. In order to differentiate the hole relaxation processes from that of $(e$-$h)$ pairs, we study in parallel the relaxation of holes in KBr doped with NO_2^-, which is known as an effective electron-trapping center.[32] A brief description of the results on KBr and KBr:NO_2^- has been given elsewhere.[31]

The paper is organized as follows. After describing experimental details in Sec. II, we present in Sec. III experimental results of the femtosecond time-resolved spectroscopy for KBr:NO_2^-, KBr, and RbBr crystals over the temperature range from 6 to 300 K. In the first part of Sec. IV, we discuss the specific features of the results which yield qualitative understanding of the relaxation process of $(e$-$h)$ pairs in bromide crystals. Then we formulate a rate-equation model for describing the temporal evolution of the states concerned, and analyze the data quantitatively. Finally we discuss some important features of relaxation processes of $(e$-$h)$ pairs in more detail, based on the experimental results and those obtained by quantitative analysis.

II. EXPERIMENT

Specimens of a thickness of 2 mm of pure KBr and RbBr were obtained from crystal blocks purchased from Harshaw Chemical Co. Those of NO_2^--doped (0.3 mol %) KBr were grown by the Kyropoulos method in dry argon atmosphere. Laser pulses of 100-fs pulse duration, 605 nm in wavelength, and 250 μJ in energy/pulse, were generated with a repetition rate of 10 Hz by a laser system comprising a mode-locked Ar-ion laser (Spectra-Physics, Model 2030), a synchronously pumped, cavity-dumped dye laser (Spectra-Physics, Model 375B) with Rhodamine 6G, a pulse compressor, and a four-stage amplifier with a Q-switched Nd:YAG laser (Continuum, Model 661-10). The second harmonic (302.5 nm) of the 100-fs laser light, generated by a KDP crystal, was used for generating $(e$-$h)$ pairs by two-photon absorption, and femtosecond white-light pulses generated by the fundamental beam in a D_2O cell were employed for probing optical absorption. The pulse width of the second harmonic was estimated to be 200 fs. The optical absorption spectra were obtained in a range between 1.3 and 3 eV by using a set of polychromators consisting of grating monochromators (Jobin Yvon, HR320) and photodiode array detectors (Princeton, RY1024) to analyze the spectra of the source beam and of the light transmitted through the specimen. The time delay of the probe pulse with respect to the incidence of the excitation pulse was controlled by an optical delay line. The absorption spectra for several lengths (l_d's) of an optical-delay line were measured, and the whole set of these spectra was used to obtain the time-resolved absorption spectrum with a given time delay t_d in the range from -10 to 150 ps by correcting for the effects of the group-velocity dispersion of the white-light pulse.

In order to obtain the absorption spectra with a reasonable signal-to-noise ratio, averaging of 5 or 10 set of data for the same l_d was needed in the present experiment. In pure crystals, the optical absorption induced by a single shot of the excitation pulse decayed almost to zero within 100 ms (the time to the incidence of the next excitation pulse), and the absorption due to stable defects was negligible.[33] Even for 20 shots at the same spot of a specimen, the amount of stable defects, mainly F centers, was at most a few percent of the maximum height of the optical absorption. Therefore, possible secondary effects due to photoexcitation of stable defects by the exciting light pulse could be neglected. However, this small amount of stable-defect absorption induced by a repeated irradiation certainly gave non-negligible effects in determining the absorption spectra at short t_d's where the absorption strengths were small. Since the amount of stable defects was confirmed to be proportional to the number N of irradiations at the same spot, the effects of the inclusion of stable-defect absorption in a measured spectrum at a given length l_d of the delay line could be subtracted by the following procedure:

$$\alpha(l_d)=\frac{1}{N}\left(\sum_{i=1}^{N}\alpha_i^{\mathrm{mes}}(l_d)-\frac{N-1}{2}\,\alpha(\infty)\right), \qquad (1)$$

where $\alpha(l_d)$ is the true absorption spectrum for a given l_d, $\alpha_i^{\mathrm{mes}}(l_d)$ the spectrum measured at ith time of the repeated irradiation, and $\alpha(\infty)$ the spectra measured after repeated irradiation, respectively. The validity of this procedure was confirmed by comparing the spectrum thus obtained with the spectrum obtained by averaging the data taken at a virgin part of the specimen by changing the sample spot for each shot of irradiation of excitation pulse; the two spectra showed no difference within experimental error. The subtraction of the stable-defect absorption in terms of Eq. (1) was applied to spectra at all l_d's. However, this procedure for obtaining the true absorption spectra was not applicable for KBr:NO_2^- at low temperatures, since the defects, the V_K centers, generated by a single shot of the excitation pulse did not

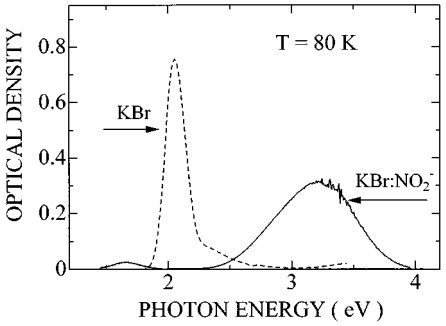

FIG. 2. Optical absorption spectra due to stable defects induced by a single shot of 1-MeV electron pulse at 80 K in pure KBr (broken curve) and KBr:NO_2^- (solid curve). Measurements were made at 80 K at 5 min after irradiation.

show any decay within 100 ms. Therefore, data could only be obtained at 273 K, where the V_K centers decayed within 100 ms.

In order to characterize the absorption bands observed in the time-resolved spectroscopy in femtosecond time regime, optical absorption bands due to typical color centers were examined at the same temperatures as those in femtosecond spectroscopy with using a pulsed-electron generator (HP 43710A) as the excitation source. The transient absorption spectra for centers which decayed within a few s after irradiation were measured by a polychromator consisting of a Xe-flash lamp, a grating monochromator and a photodiode array detector. The absorption bands due to stable defects were measured by a conventional spectrophotometer (Shimadzu UV3100).

III. EXPERIMENTAL RESULTS

First, in order to confirm that the relaxation of holes takes place without any significant interaction with electrons in KBr:NO_2^-, we measured optical absorption spectra after irradiation with a single shot of a 20-ns electron pulse at 80 K. Figure 2 shows the absorption spectra measured a few min after irradiation for pure KBr and KBr:NO_2^-. It is evident that in doped specimens the induced absorption bands are entirely due to V_K centers, whereas only F bands are generated in pure KBr. When the absorption spectrum was measured 100 ns after irradiation, the induced absorption bands were identical to those measured a few min after irradiation; no transient species could be detected in KBr:NO_2^-. On the other hand, the optical absorption bands due to the off-center STE's, as well as F and H bands, were produced in pure KBr at 6 and 80 K. Therefore, it is clear that the holes are relaxed without interaction with electrons in the KBr:NO_2^- crystals.

In Fig. 3 we compare the time-resolved optical absorption spectra for (a) KBr:NO_2^- at 273 K and for (b) pure KBr at 80 K after irradiation with a femtosecond laser pulse; the delay t_d of the probe pulse is indicated at each panel. In the top panels the V_K bands in KBr:NO_2^- measured at 273 K and the absorption bands due to the off-center STE, the STE band, and the F band in pure KBr at 8 K generated by pulse-electron irradiation are shown for comparison. The time-resolved spectra in both specimens before 1.6 ps are similar; only a broadband extending over the whole photon-energy

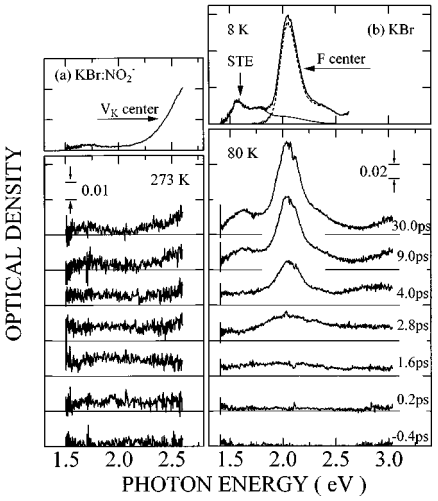

FIG. 3. Time series of optical absorption spectra for (a) KBr:NO_2^- at 273 K, and for (b) pure KBr at 80 K; the probe pulse delay is given in each panel. The top panels of (a) and (b) show, respectively, the V_K band measured at 273 K and the transient absorption spectrum in pure KBr measured at 1 μs after an electron-pulse irradiation at 8 K. The V_K band at 273 K was measured at 10 μs after irradiation of an electron pulse, since the V_K center is not stable at this temperature. The transient absorption spectrum in pure KBr is decomposed into the STE band (thin solid curve) and the F band (broken curve).

range is observed. Hereafter we call this band the B band. However, a significant difference is evident in the spectra after 2.8 ps: the F band at 2.05 eV and the STE band at 1.6 eV are generated in pure KBr, while in KBr:NO_2^- the B band converges to at least two peaks at 1.7 and $>$2.6 eV. Although we were able to detect only the tail of the optical absorption band with photon energies smaller than 2.6 eV, we believe that this spectrum corresponds to the V_K center which has two maxima at 1.7 and 3.2 eV.

The time evolution of the optical absorption measured at 2.5 and 2.0 eV in KBr:NO_2^- is shown in Figs. 4(a) and 4(b); the latter monitors almost purely the B band and the former includes the contributions from both the B band and the V_K band. The B band reaches a maximum at 1.5 ps after excitation, and decays within 10 ps. The long-lived component in Fig. 4(a) can be ascribed to V_K centers. From these results, it is clear that the formation of the V_K center is delayed by about 10 ps after generation of free holes. Evidently the delay of the V_K-center formation has a close correlation with the formation of transient hole centers which exhibits the B band. The solid curves in Figs. 4(a) and 4(b) represent the results of analysis based on the rate-equation model, which is described in detail in Sec. IV B.

In Figs. 4(c)–4(e), we show the time evolution of the optical absorption measured at 1.92, 1.60, and 1.33 eV in pure KBr, respectively. In these figures, the solid curves are the results of analysis. The optical absorption measured at 1.92 eV is mostly due to the F band as seen in Fig. 3(b). Clearly two processes determine the growth of the F band: a fast process occurs within 6 ps, and a slow one continues over 50 ps at 80 K. Neither process is due to electron trapping by preexisting anion vacancies:[33] they are indicative of the formation of Frenkel pairs from $(e\text{-}h)$ pairs. The tempo-

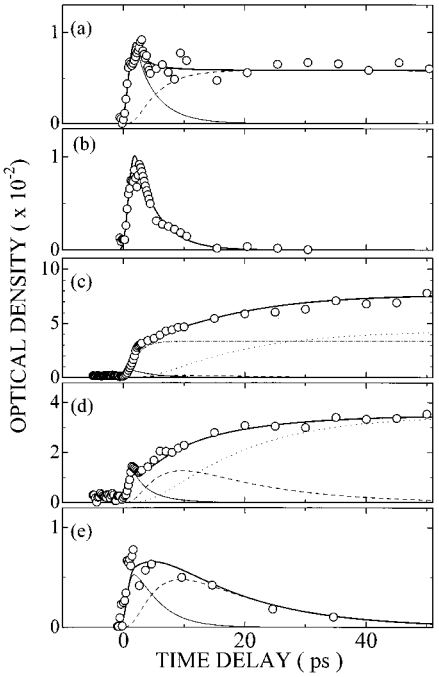

FIG. 4. Optical density changes at (a) 2.5 eV and (b) 2.0 eV in KBr:NO_2^- at 273 K and (c) 1.92 eV, (d) 1.60 eV, and (e) 1.33 eV in pure KBr at 80 K as a function of delay after two-photon band-to-band excitation. The solid curves pertaining data points are the results of analysis by using a rate-equation model (see the text). Thin solid curves in (a) and (b) show the temporal evolution of the B band, and the broken curve in (a) shows the growth of the V_K band. In (c), (d), and (e), thin solid and broken curves show the temporal evolution of the B band and the absorption band due to intermediate state I, respectively. The chain and dotted curves in (c) show the two components of the temporal evolution of the F band, and the dotted curve in (d) shows that of the STE band.

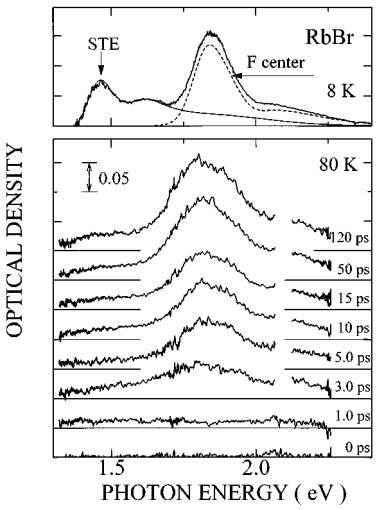

FIG. 5. Time series of optical absorption spectra for RbBr at 80 K; the probe pulse delay is given in each panel. The top panel shows the transient absorption spectrum measured at 1 μs after an electron-pulse irradiation at 8 K. The transient absorption spectrum is decomposed into the STE band (thin solid curve) and the F band (broken curve).

ral evolution of the slow growth of the F band is well described by a function of the form $[1-\exp(-t/\tau)]$, with $\tau=13$ ps.

In contrast to the growth of the F band, the growth of the STE band includes only the slow component; the apparent fast growth at 1.60 eV in Fig. 4(d) is not due to the STE band but is primarily due to the B band as evidenced by the time-resolved spectra shown in Fig. 3(b). The growth of the STE band is found to be parallel to the slow growth of the F band. On the other hand, the evolution of the optical absorption at 1.33 eV shown in Fig. 4(e) demonstrates a rapid growth within 5 ps and slow decay lasting for 50 ps. Comparing these time-resolved spectra with those in KBr:NO_2^-, they can be divided into two components: one that behaves similarly to the B band and another which grows more slowly and is not annihilated completely for 50 ps. The latter component is absent in KBr:NO_2^-, and is seen only in pure KBr. The time constant of the decay of this component is found to be about 13 ps, identical to those of the slow growths of the F band and of the STE band. Therefore, an intermediate state, hereafter called state I, is formed within 5–6 ps after excitation in pure KBr, and the decay of state I is related to the formation of the F centers at the slow process and of the off-center STE's.

Figure 5 shows the time-resolved optical absorption spectra for pure RbBr at 80 K after irradiation with a femtosecond laser pulse. The delay of the probe pulse with respect to the excitation pulse is indicated in each panel. In the top panels the STE band and F band in RbBr generated by pulse-electron irradiation at 8 K are shown for comparison. The features of the time-resolved spectra for RbBr are quite similar to those for KBr; only a broadband extending over the whole photon-energy range is observed at early t_d's, the F band at 1.80 eV is then induced at t_d of 3 ps, and for t_d's longer than 10 ps the F band and the STE band at 1.45 eV are generated.

The time evolution of the optical absorption at 1.38, 1.50, and 1.85 eV in RbBr are shown in Figs. 6(a)–6(c), respectively. The optical density measured at 1.85 eV is mostly due to the F band, as evidenced in the time-resolved spectra shown in Fig. 5. As in the case of KBr two processes in the growth of the F band are evident; a fast growth that occurs within 6 ps and a slow one that continues over 80 ps at 80 K. The changes in optical density at 1.38 eV at which the contribution of the STE's is significant show a rapid growth followed by a fast decay within 6 ps, and a gradual increase that continues over 80 ps. In view of the time-resolved absorption spectra in Fig. 5, it is clear that the rapid changes at short t_d's are due to the generation and annihilation of the B band, and the gradual increase is due to the growth of the STE bands. The changes at 1.50 eV, where the contribution of the STE band is more than at 1.38 eV, are also characterized by fast changes at less than 6 ps and a gradual increase at longer t_d's. Since the absorption peaks of the F centers and STE's in RbBr are at lower energies than those in KBr, the optical density changes corresponding to those at 1.33 eV in KBr could not be detected in the wavelength range of the present detector.

In order to examine the effects of temperature on the relaxation process of $(e\text{-}h)$ pairs in KBr and RbBr, we carried out similar time-resolved optical absorption measurements over a wide temperature range, from 6 to 300 K. In Fig. 7,

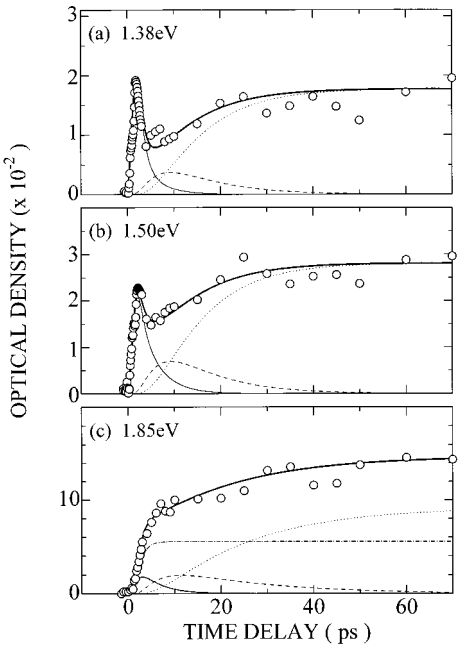

FIG. 6. Optical density changes at (a) 1.38 eV, (b) 1.50 eV, and (c) 1.85 eV in pure RbBr at 80 K as a function of delay after two-photon band-to-band excitation. The solid curves pertaining to data points are the results of analysis by using a rate-equation model (see the text). In the figures, thin solid and broken curves show the temporal evolution of the *B* band and the absorption band due to the intermediate state *I*, respectively. The dotted curves in (a) and (b) show the temporal evolution of the STE band, and the chain and dotted curves in (c) show the two components of the temporal evolution of the *F* band.

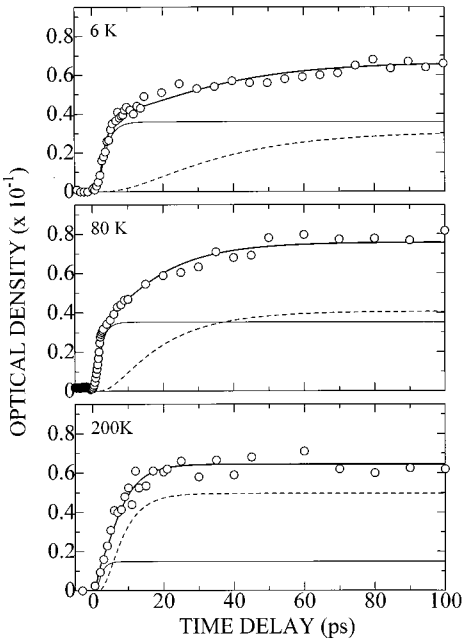

FIG. 7. Optical density changes at 2.0 eV in pure KBr at 6, 80, and 200 K as a function of delay after two-photon band-to-band excitation. The solid curves are the results of analysis by using a rate-equation model (see the text). The temporal evolution of the fast and slow growth of the *F* band, resolved by the analysis, are shown by thin solid and broken curves, respectively.

we show time evolution of optical densities at 2.0 eV at 6, 80, and 200 K in KBr, which monitors changes in the concentration of *F* centers. The results at 80 K, which were already shown in Fig. 4, are again presented to emphasize the temperature dependence. At 6 K, the presence of two processes in the *F* band growth demonstrated at 80 K is clearer, because of the much slower time constant at the second stage after 6 ps. The slow growth at the second stage was also found in the optical density changes at 1.6 eV. On the other hand, at 200 K there appears to be a ''single-mode'' growth; the optical density increases continuously until 20 ps, and then stays almost constant at longer t_d's. The change at 1.6 eV (the STE absorption band) also shows a ''single-mode'' growth until 20 ps, and then starts to decrease at longer t_d's at this temperature. The growth of the *F* band measured at 300 K was found to be similar to that at 200 K, except for a slightly shorter rise time.

Figure 8 shows the results of temporal evolution of the *F* band monitored at 1.85 eV at 6, 80, and 200 K in RbBr. The effects of temperature on the growth kinetics of the *F* band in RbBr are similar to those in KBr. At 6 K, the fast growth within 6 ps is dominant; the slow increase at longer t_d's certainly exists, but is much smaller than that in the first stage. At 200 K, the growth of the *F* band appears to occur via a ''single mode;'' it increases monotonically until 30 ps. It appears that the formation time of the *F* center is slower at 200 K than at 5 K.

As seen in Fig. 7, at any temperature from 6 to 300 K, the formation of *F* centers in KBr is completed within around 100 ps. We examined the temperature dependence of the yield of *F* centers measured at 120 ps after excitation with the femtosecond light pulse; the area of the *F* band induced at each temperature was measured as a function of the temperature. It was found that the yield of *F* centers in KBr was almost constant irrespective of the temperature from 6 to 300 K. This temperature independence of the fraction of $(e\text{-}h)$ pairs which are relaxed into $F\text{-}H$ pairs suggests strongly that observed temperature dependence of the time evolution of the *F* band reflects that of the relaxation pathways of $(e\text{-}h)$ pairs. The origin of this temperature dependence will be discussed in the next section.

IV. DISCUSSION

A. Characteristic features of the relaxation process of $(e\text{-}h)$ pair

The relaxation of $(e\text{-}h)$ pairs in KBr and RbBr described in the previous section can be qualitatively divided into two stages: a first stage that terminates within 6 ps, and the second stage which follows the first stage and continues over 100 ps at low temperatures. The first stage is characterized by three features: (1) the rapid growth and decay of the *B* band, (2) the fast evolution of the *F* band, and (3) formation of the intermediate state *I*. The second stage is characterized by the decay of the intermediate state *I*, which is formed at the first stage, and the slow growth of the *F* band and the STE band. Here we discuss these results in more detail to obtain qualitative understanding of the lattice relaxation which takes place in each stage.

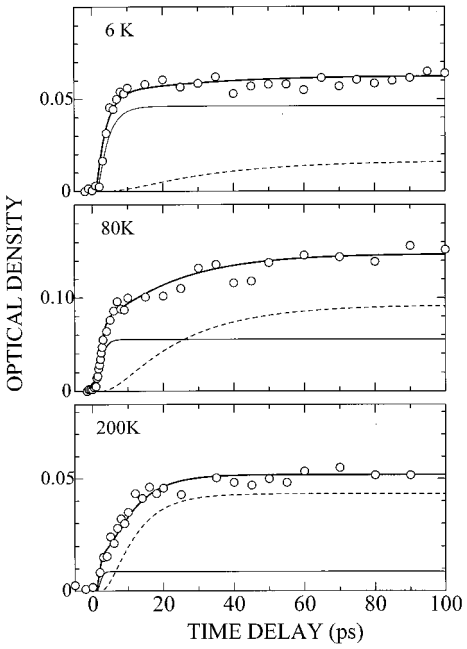

FIG. 8. Optical density changes at 1.85 eV in pure RbBr at 6, 80, and 200 K as a function of delay after two-photon band-to-band excitation. The solid curves are the results of analysis by using a rate-equation model (see the text). The temporal evolution of the fast and slow growth of the F band, resolved by the analysis are shown by thin solid and broken curves, respectively.

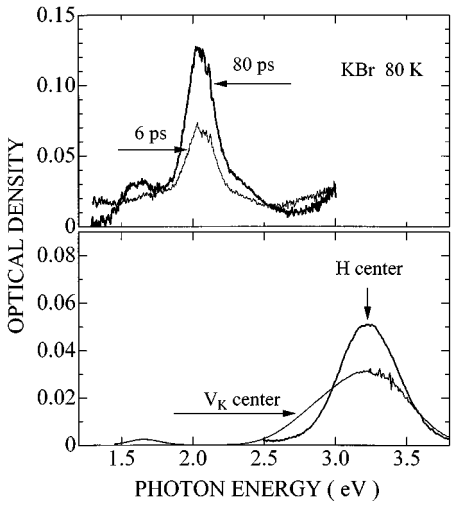

FIG. 9. (a) The time-resolved absorption spectra at 6 and 80 ps after two-photon band-to-band excitation in KBr at 80 K, and (b) the absorption spectra due to V_K and H centers in KBr. The spectrum due to H centers was measured at 10 μs after an electron-pulse irradiation at 80 K, since the center is not stable above 40 K.

1. The lattice relaxation at the second stage: The off-center relaxation

Since the decay time constant of the state I, monitored at 1.33 eV in KBr, is identical to the time constant of the growth of the F and STE bands, we can preliminarily conclude that the second stage of the relaxation is due to the conversion of the state I into F-H pairs and off-center STE's. In order to get deeper insight into this second stage of relaxation, let us examine closely the changes in optical absorption spectra for KBr. In Fig. 9(a), we compare the spectra at t_d's of 6 and 80 ps measured at 80 K. Three prominent features can easily be noticed; the decay of the absorption at photon energies below 1.4 eV, the growth of the F and STE bands and the significant ''sharpening'' of the absorption band above 2.5 eV. From previous optical-absorption spectroscopy studies of color centers, it is well established that the absorption around 3 eV at low temperatures arises mainly from X_2^- molecular ion centers.[34] In pure crystals, these are V_K and H centers. In Fig. 9(b), we compare the absorption bands of the V_K and H centers measured at 80 K. Although both centers have peaks around 3.2 eV, the band is much broader and shows a low-energy tail in the case of the V_K center.[20,35] The absorption band above 2.5 eV at 6 ps fits the V_K-absorption band almost perfectly, whereas that at 80 ps fits the H-absorption band. Therefore, the intermediate state I in pure KBr is characterized by an absorption band similar to that of the V_K center at energies above 2.5 eV. It is also clear that state I exhibits a significant absorption strength below 1.5 eV. These spectroscopic features are characteristic to the type-I STE in alkali halides[18] which has been shown to have the on-center configuration.[17] Thus we can assign the intermediate state I to the on-center STE. It follows then that the second stage of the relaxation can be understood as the off-center relaxation of the on-center STE into the F-H pair and the off-center STE. Further details of this relaxation will be discussed after quantitative analysis of the data.

2. The lattice relaxation at the first stage: The dynamical relaxation of a complex comprising an electron and a relaxing hole

One of the striking features of the present results is that the F-H pairs are generated not only through the slow process described above, but also through the fast process within 6 ps. From the results for KBr:NO_2^-, it is evident that the hole relaxation into the V_K center is completed at around 10 ps after excitation. Therefore, the holes well before 10 ps can be considered as still being in the process of relaxation.[36] The transient hole centers which give rise to the B band can be identified to be these holes in the process of relaxation, and they are called hereafter the relaxing holes. Since the relaxation at various lattice sites where holes are localized is not in phase, it is reasonable to assume that the relaxing holes can give rise to a broad optical absorption band. The result that the broad B band transforms into the V_K band in KBr:NO_2^- is totally consistent with this interpretation. In pure crystals, however, the relaxing holes will start to interact with electrons at some stages of their relaxation. Then, the fast formation of the F-H pair taking place within 6 ps after excitation is ascribed to the interaction of electrons with relaxing holes. As the on-center STE is also formed in this first stage of relaxation, we may conclude that the interaction of an electron with the relaxing hole evolves by two different pathways: one leading to formation of the F-H pair, and another leading to the on-center STE.

Most existing models[4,23–28] of Frenkel-pair formation from an exciton or an $(e$-$h)$ pair proposed so far assume that the hole relaxation into the V_K center is the primary step; any further relaxation occurs after the hole self-trapping into the V_K-center configuration is completed. The F-H pair forma-

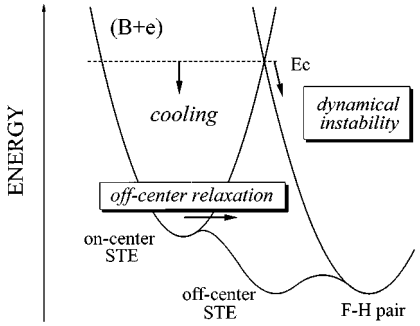

FIG. 10. The schematic configuration coordinate diagram showing the model of relaxation pathways of $(e\text{-}h)$ pairs in KBr and RbBr. $(B+e)$ stands for the state comprising an electron and a relaxing hole. Arrows show possible relaxation routes (see the text).

tion in the second stage observed in this study has provided the first direct evidence for the model proposed in Ref. 28. At the same time, however, the present investigation has revealed a new direct channel of $F\text{-}H$ pair generation due to the interaction of electrons with relaxing holes. The instability induced at this stage of relaxation can be reasonably referred to as a dynamical instability in the sense that it is induced during lattice relaxation of $(e\text{-}h)$ pairs which is associated with violent motions of ions. The existence of this channel has provided evidence for the dynamical interplay of the electron-lattice and hole-lattice interaction inducing local lattice rearrangements.

3. Relaxation pathways of (e-h) pairs

Based on the results and discussions described above, it can be concluded that the relaxation of $(e\text{-}h)$ pairs in KBr and RbBr is characterized by the following pathways. In the first stage of relaxation, optically generated holes are localized to form the relaxing holes, and the interaction of electrons with the holes in pure crystals results in the formation of either $F\text{-}H$ pairs or the on-center STE. In the second stage of relaxation at longer t_d's, the on-center STE formed in the first stage is converted into either $F\text{-}H$ pair or the off-center STE through off-center relaxation. These pathways can be represented schematically by the configuration coordinate diagram shown in Fig. 10.

In this figure, the complex comprising an electron and a relaxing hole, abbreviated as $(B+e)$, is taken to be the ''vibrationally'' excited state of the on-center STE; the vibrational relaxation of the complex eventually leads to the formation of the on-center STE. This assignment is based on our results for KBr:NO_2^- in which the decay of the relaxing holes leads to the formation of the V_K centers. Direct conversion into $F\text{-}H$ pair configuration due to dynamical instability is also shown as a relaxation pathway of $(B+e)$. The model shown in Fig. 10 includes two assumptions which are not evident from the above discussion. The first is that the dynamical instability takes place at a certain excited state of $(B+e)$ with an excess energy around E_c, and the second is the existence of a barrier between the on-center STE and the off-center STE. The validity and physical significance of these assumptions will be discussed in Secs. IV C and IV D.

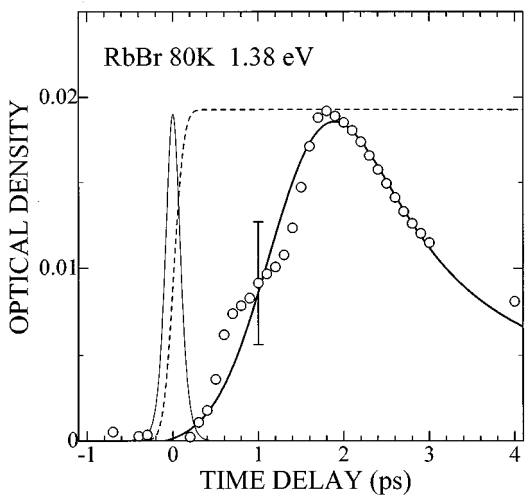

FIG. 11. Optical-density changes at 1.38 eV in RbBr as a function of time delay after two-photon band-to-band excitation at 80 K. The thin solid curve shows the pulse shape (200-fs width) of the excitation pulse with a hyperbolic-secant-squared form, and the broken curve shows the convoluted rise of the absorption with no delay. The pulse width of 100 fs for the probe pulse was used for the convolution analysis. The thick solid curve pertaining to data points is the result of the analysis using a rate-equation model in which a generation function of a Gaussian form is used (see the text).

B. Analysis of the time evolution in terms of a rate-equation model

To characterize the relaxation process of $(e\text{-}h)$ pairs in quantitative terms, we analyze the temporal evolution of several absorption bands by introducing a system of rate equations based on the model of the relaxation proposed in Fig. 10. First we describe some features of the rate-equation model used.

1. Introduction of the generation function of the B state

As described in Sec. III, the fastest process observed in optical absorption is the generation of the B band corresponding to relaxing holes. In Fig. 11, we show on an extended time scale the temporal evolution of the optical density at 1.38 eV in RbBr which is determined predominantly by the B band. The shape of the excitation pulse is shown by the thin solid line, and the convoluted rise calculated numerically using a hyperbolic-secant-squared shape of the excitation and probe pulses in the case of zero delay of the formation is shown by the broken curve. It is evident that the convoluted rise curve does not fit the growth of the B band; there is a delay in the formation of the B band. Thus, we are forced to introduce some transient states responsible for the formation of the B band; these are not presently detectable experimentally.

We assume that the formation of the transient hole centers or the relaxing holes does not happen in a single step, but includes several distinct steps, such as the cooling of optically generated hot holes through successive scattering with phonons within the valence band and localization through interaction with a randomly fluctuating lattice potential. Therefore, it is reasonable to assume that a wide distribution

for the time needed for an optically generated hole to be localized at a certain lattice site with a certain degree of relaxation. Also, it has been shown that the relaxation which occurs in the subpicosecond time regime includes dynamical features which can be described by wave-packet dynamics.[29] When we take these features of the lattice relaxation of holes into account, the consideration of a transient state with a fixed decay constant is too simple to simulate the process.

Here we introduce a generation function $g(t)$ of the relaxing hole state to describe the fact that the population of the state after creation of $(e\text{-}h)$ pairs is distributed with respect to the time delay after excitation. The function is given by

$$g(t)=\exp\left(-\frac{(t-t_0)^2}{w^2}\right), \tag{2}$$

and is characterized by the overall delay t_0 and the distribution half width $w/\sqrt{4\ln 2}$. The distribution of the formation time described by $g(t)$ can be regarded as a phenomenological representation of the dephasing effects and of a convolution of the unresolved primary steps in the hole-relaxation process. In Fig. 11, the thick solid curve is calculated with $g(t)$ by fitting a rate-equation model, details of which are given below, to the data. In this fitting, $t_0=1.1$ ps and $w=0.8$ ps were used. It is evident the introduction of the generation function significantly improves the description of the temporal evolution of the B band.

2. Rate equations

For constructing the set of rate equations, we need to specify the relation between the two relaxation channels of $(B+e)$, the formation of the F-H pair and the on-center STE. If any of the $(B+e)$ states has the same probability of decay into either of the these two states, the formation time of the F band and the decay time of the B band is identical. However, we find in the experimental results and in the fitting procedure that the formation time of the F band is usually shorter than the decay time of the B band in both KBr and RbBr. This can be interpreted as indication that among many substates of $(B+e)$ with distributed degrees of relaxation, only some specific states can be responsible for decomposition into F-H pairs. Therefore, we introduce two distinct levels of $(B+e)$: the $(B+e)_{\boldsymbol{l}}$ level has only one channel of relaxation into the on-center STE, and the $(B+e)_{\mathbf{h}}$ level is responsible for both the conversion into the F-H pairs through the fast process and the relaxation into the $(B+e)_{\mathbf{1}}$. It follows that competition between the two channels of the relaxation of the $(B+e)$ takes place at the level $(B+e)_{\mathbf{h}}$, and the branching ratio is characterized by the rate k_h^F of the dynamical transfer into the F-H pair and the rate k_h^ν of the vibrational relaxation towards the lower states at $(B+e)_{\mathbf{h}}$. The formation time of the F-H pair is then given by $1/(k_h^F+k_h^\nu)$. On the other hand, the decay of the B band may be characterized by a rate of vibrational relaxation averaged by many lower levels. Since the rate is lower for lower-energy levels, the time constant of the decay of the B band is expected to be larger than $1/k_h^\nu$, and hence $1/(k_h^F+k_h^\nu)$. When two different levels for $(B+e)$ are introduced, then the decay of the B band is finally governed by the lifetime $1/k_l^\nu$ of the $(B+e)_{\boldsymbol{l}}$ level.

Now one can construct the set of rate equations to simulate the time evolution of each absorption band. The arrows in Fig. 10 indicate the overall transition routes from one level (i) to the others (j). The rates of these transitions are here represented by k_i^j. The rate equations for levels concerned are given by

$$\frac{dn_h}{dt}=g(t)-(k_h^F+k_h^\nu)n_h, \tag{3}$$

$$\frac{dn_l}{dt}=k_h^\nu n_h-k_l^\nu n_l, \tag{4}$$

$$\frac{dn_I}{dt}=k_l^\nu n_I-(k_I^F+k_I^S)n_I, \tag{5}$$

$$\frac{dn_S}{dt}=k_I^S n_I, \tag{6}$$

$$\frac{dn_F}{dt}=k_h^F n_h+k_I^F n_I, \tag{7}$$

where n_i $(i=h,l,I,S,F)$ represents, respectively, the concentrations at $(B+e)_{\boldsymbol{h}}$, $(B+e)_{\boldsymbol{l}}$ the on-center STE, the off-center STE, and the F-H pair. This set of rate equations was solved numerically, using a fourth-order Runge-Kutta algorithm, to fit to the temporal evolution of optical densities at typical photon energies. In the fitting procedure, consistent values of parameters of t_0 and w were used for a given specimen at all photon energies. The solid curves shown in Figs. 4, 6, 7, 8, and 11 which represent the results of the best fit, demonstrate that our analysis in terms of the rate-equation model reproduces reasonably the temporal evolution of optical densities at several photon energies.

The components resolved by the analysis show some characteristic temperature dependence which reflects that of the relaxation pathways of $(e\text{-}h)$ pairs. As one can see in Figs. 7 and 8, as the temperature increases the amount of F centers formed through the fast process in the first stage is reduced, whereas that amount through the slow process in the second stage is enhanced. Simultaneously, the rise time of the F band in the second stage is becoming shorter with increasing temperature. These two features related to the F-center formation are discussed in the next section.

C. Temperature dependence of the yields of F centers in the two stages: The competition between the two pathways during relaxation of the $(B+e)$ state

According to the model in Fig. 10, the fast process of the F-center formation in the first stage results from the interaction between electron and relaxing hole, and the slow process in the second stage is due to the off-center relaxation of the on-center STE. In terms of the rate of the relaxation, the amount η_F^f of the F centers formed in the fast process is given by

$$\eta_F^f=\frac{k_h^F}{k_h^F+k_h^\nu}, \tag{8}$$

and, the amount η_F^s of the F centers formed in the slow process is given by

$$\eta_F^s = \frac{k_h^\nu}{k_h^F + k_h^\nu} \times \frac{k_I^F}{k_I^F + k_I^S}. \tag{9}$$

Therefore, the result that the amount of the F centers formed in the fast process is replaced by almost the same amount in the slow process at higher temperature means that the vibrational relaxation leading to the on-center STE becomes dominant over the direct transfer into the F-H pair state at higher temperatures.

The problem of the competition between a dynamical transition from an excited state to an other state and the vibrational relaxation within the excited state has been studied both experimentally and theoretically for several systems in solids.[37–40] A typical example is the Dexter-Klick-Russell mechanism[37] for radiationless transitions in the F centers, where the dynamical transition to the ground state and the cooling transition within the excited state manifold are the two processes concerned. Following the theoretical concept of Bartram and Stoneham,[39] the $(B+e)$ state we are concerned with may be described as a vibrationally excited state in the configuration coordinate space spanned by the ''effective local mode,'' or the interaction mode.[41] The vibrational relaxation is then governed by the interaction between the effective local mode and the ''effective lattice modes'' which act as a reservoir. It has been shown[39] that the cooling transition rate k_h^ν of the nth vibrational state on the interaction-mode space is given approximately by

$$k_h^\nu = k_0 n_r (2n+1) \tag{10}$$

for $n_r \gg 1$, where k_0 is a constant and n, which is given by

$$n = [\exp(h\nu/kT) - 1]^{-1}, \tag{11}$$

is the occupation number of the effective lattice mode at temperature T with the simplification of representing the lattice by a single mode. Then, the rate k_h^ν increases with increasing temperature. If we assume that the rate k_h^F of the direct transfer into the F-H pair state is not very sensitive to temperature, then the temperature-dependent decrease of the amount of F centers formed in the fast process can be one of direct consequences of our model of the relaxation.

The relative yield of η_F^f to the total yield of the F centers is given by

$$\frac{\eta_F^f}{\eta_F^f + \eta_F^s} = \frac{k_h^F}{k_h^F + c k_h^\nu}, \tag{12}$$

where $c = k_I^F/(k_I^F + k_I^S)$. In Fig. 12, we plot the relative yield determined by analyzing the results, and show the best fit curve of Eq. (12), with the aid of Eqs. (10) and (11), with $h\nu$ as a fitting parameter. In this fitting, we assumed c to be independent on temperature. This assumption could be verified by the results of analysis; the magnitude of c for obtaining the best fit at different temperatures changes by less than 10%. As seen in the figure, Eq. (12) describes well the temperature dependence of the relative yield of η_F^f in both KBr and RbBr. The analysis and arguments described here may substantiate our assumption that the dynamical instability takes place at a certain excited state of $(B+e)$ with competing with the cooling transition into the on-center STE.

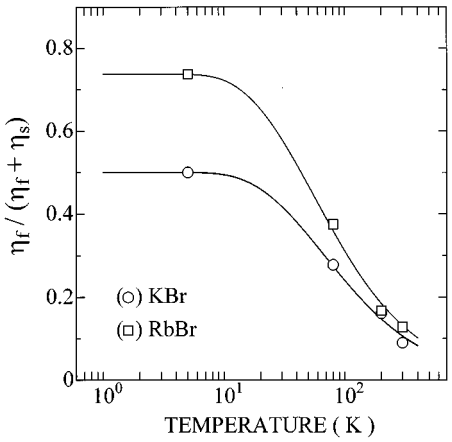

FIG. 12. The relative yield of the F centers formed at the first stage to the total yield of the F centers in KBr and RbBr as a function of temperature. The solid curves are the results of the best-fit of Eq. (12).

D. Temperature dependence of the formation time of the F center in the slow process: The barrier against the off-center relaxation of the on-center STE

As concluded in Sec. IV A, the second stage of the relaxation of $(e$-$h)$ pairs is the off-center relaxation from the on-center STE into the F-H pair and the off-center STE. The analysis has shown that the relaxation is characterized by a single time constant, which depends on temperature and also on the crystal. In Fig. 13, we plot the time constant τ_I $[=1/(k_I^F + k_I^S)]$, namely the rise time of the F band at the second stage, as a function of temperature for KBr and RbBr. It is evident that τ_I which remains constant at low temperatures has become shorter with increasing temperature. We apply the classical formula for the nonradiative transition probability:

$$\frac{1}{\tau_I} = k_I^0 + \nu \exp(-E/k_B T), \tag{13}$$

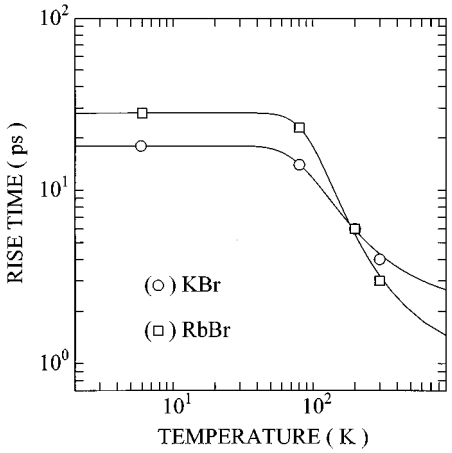

FIG. 13. Temperature dependence of the rise time of the F band at the second stage in KBr and RbBr. The solid curves are the best fit of Eq. (13).

where k_I^0 is the rate of low-temperature tunneling, k_B the Boltzmann constant, and ν and E are the frequency factor and the activation energy of the thermally activated process, respectively. The temperature dependence of τ_I can be fitted well by Eq. (13). The solid curves in Fig. 13 are the best fits for the two bromide crystals. The fitted values of E are 29 and 37 meV for KBr and RbBr, respectively. The result that the rate of the off-center relaxation increases with increasing temperature, described well by Eq. (13), indicates that there is a barrier between the on- and off-center configurations of the STE's. Therefore, the present study has demonstrated clearly the bistability of the two different relaxed configurations of excitons.

The off-center instability of the on-center configuration of the STE in alkali halides was first studied theoretically by Toyozawa,[4] and he proposed that at a certain amount of distortion of the symmetric vibrational mode, Q_1 mode, of the X_2^- molecular ion, the pseudo-Jahn Teller effects of $1s$- and $2p$-like electronic states due to an odd-parity mode, Q_2 mode, of X_2^- molecular ion induces the instability to displace the molecular ion into a $\langle 110 \rangle$ direction. Later, Toyozawa's concept was quantitatively analyzed in detail by Leung and Song.[42] However, in a model which assumes linear coupling between the electronic system and the Q_1- and Q_2-mode vibrations, the double-minima structure of the adiabatic potential-energy surface cannot be formed, as analyzed in detail by Matsumoto, Shirai, and Kan'no.[43] Cluster calculation by several methods, including the *ab initio* approach, has shown that the off-center instability is certainly favored, but most of these theoretical studies have failed to show satisfactorily the bistability, i.e., the presence of a barrier between the on- and off-center configurations of STE's.[15,28,44–48] Thus, the bistability of the two different configurations of STE's remains a challenge for future theoretical studies with more sophisticated methods, as discussed in Ref. 48.

V. SUMMARY

We have studied the dynamics of relaxation of $(e\text{-}h)$ pairs in KBr and RbBr using femtosecond time-resolved spectroscopic technique. Several primary processes of the relaxation have been resolved for the first time. In both KBr and RbBr, the relaxation process of $(e\text{-}h)$ pairs has been resolved into two distinctive stages. In the first stage which terminates within 5–6 ps after excitation, the interaction of electrons with relaxing holes leads to the formation of $F\text{-}H$ pairs and to the on-center STE. The branching between the two channels of the relaxation is temperature dependent; the yield of $F\text{-}H$ pairs formed in this first stage is reduced at higher temperature. The temperature-dependent branching has been ascribed to the temperature-enhanced rate of the cooling transition of the complex consisting of an electron and a relaxing hole. The second stage of the relaxation has been proven to be the off-center relaxation in which the on-center STE formed in the first stage undergoes further relaxation into $F\text{-}H$ pairs and the off-center STE's. The rate of this off-center relaxation has been shown to be also temperature dependent, providing evidence for the barrier between on- and off-center configurations of STE's.

These new findings, though specific to KBr and RbBr at this moment, have given important information for understanding lattice relaxation processes of elementary excitations in solids with strong electron-phonon coupling. The specimens used in this study are typical examples of alkali-halide crystals in which on- and off-center STE's can coexist. It is an interesting future problem to study how the characteristic features of the relaxation process observed in these crystals change in other alkali halides where only one type of STE can be formed, and in other crystals which have different bonding nature and crystal structures.

ACKNOWLEDGMENTS

We wish to thank Dr. K. Kan'no for his help in growing doped specimens. The authors are grateful to Professor N. Itoh, Dr. A. Shluger, and Professor A. Nakamura for valuable discussions and to Dr. T. Harker for valuable comments on the manuscript. This work was supported by a Grant-in-Aid by the Ministry of Education, Culture and Science of Japan.

[1] M. Ueta, H. Kanzaki, K. Kobayashi, Y. Toyozawa, and E. Hanamura, *Excitonic Processes in Solids* (Springer, Berlin, 1986).

[2] A. K. S. Song and R. T. Williams, *Self-Trapped Excitons* (Springer, Berlin, 1993).

[3] N. Itoh, Adv. Phys. **31**, 491 (1982).

[4] Y. Toyozawa, J. Phys. Soc. Jpn. **44**, 482 (1978).

[5] N. Itoh and K. Tanimura, J. Phys. Chem. Solids, **51**, 717 (1990).

[6] *Desorption Induced by Electronic Transition*, edited by A. R. Burns, E. B. Stechel, and D. R. Jennison (Springer, Berlin, 1993).

[7] *Amorphous Semiconductors*, edited by M. H. Brodsky (Springer, Berlin, 1985).

[8] S. Koshihara, Y. Tokura, T. Mitani, G. Saito, and T. Koda, Phys. Rev. B **42**, 6853 (1990); S. Koshihara, Y. Tokura, K. Takeda, and T. Koda, Phys. Rev. Lett. **68**, 1148 (1992).

[9] N. Itoh and T. Nakayama, Phys. Lett. **92A**, 471 (1982).

[10] P. W. Anderson, Phys. Rev. Lett. **34**, 953 (1975).

[11] Y. Toyozawa, Solid State Commun. **84**, 255 (1992).

[12] W. Kanzig, Phys. Rev. **99**, 1890 (1955); T. G. Castner and W. Kanzig, J. Phys. Chem. Solids **3**, 178 (1957).

[13] K. Kan'no, K. Tanaka, and T. Hayashi, Rev. Solid State Sci. **4**, 383 (1990).

[14] K. Tanimura and N. Itoh, Phys. Rev. B **45**, 1432 (1992).

[15] C. H. Leung, G. B. Brunet, and K. S. Song, J. Phys. C **18**, 4459 (1985).

[16] T. Suzuki, K. Tanimura, and N. Itoh, Phys. Rev. B **48**, 9298 (1993).

[17] T. Suzuki, K. Tanimura, and N. Itoh, Phys. Rev. B **49**, 7233 (1994); K. Tanimura, T. Suzuki, and N. Itoh, Phys. Rev. Lett. **68**, 635 (1992).

[18] S. Hirota, K. Edamatsu, and M. Hirai, Phys. Rev. Lett. **67**, 3283 (1991); K. Edamatsu, M. Sumita, S. Hirota, and M. Hirai, Phys. Rev. B **47**, 6747 (1993).

[19] M. N. Kabler, Phys. Rev. **136**, A1296 (1964).
[20] W. Meise, U. Rogulis, F. K. Koschnich, K. S. Song, and J. H. Spaeth, J. Phys. Condens. Matter **6**, 1815 (1994).
[21] R. T. Williams, Opt. Eng. **28**, 1024 (1989).
[22] M. Hirai, in *Defect Processes Induced by Electronic Excitation in Insulators*, edited by N. Itoh (World Scientific, Singapore, 1989), p. 120.
[23] D. Pooley, Proc. Phys. Soc. **87**, 245 (1966).
[24] H. N. Hersh, Phys. Rev. **148**, 928 (1966).
[25] N. Itoh and M. Saidoh, J. Phys. (Paris) Colloq. **34**, C9-101 (1973); N. Itoh, A. M. Stoneham, and A. H. Harker, J. Phys. Soc. Jpn. **49**, 1364 (1980).
[26] M. N. Kabler, in *Proceedings for NATO Advanced Study Institute on Radiation Damage Processes in Materials*, edited by C. H. S. Dupuy (Noordhoff, Leyden, 1975), p. 176.
[27] M. N. Kabler and R. T. Williams, Phys. Rev. B **18**, 1948 (1978).
[28] R. T. Williams, K. S. Song, W. L. Faust, and C. H. Leung, Phys. Rev. B **33**, 7232 (1986).
[29] T. Tokizaki, T. Makimura, H. Akiyama, A. Nakamura, K. Tanimura, and N. Itoh, Phys. Rev. Lett. **67**, 2701 (1991); T. Makimura, K. Tanimura, N. Itoh, T. Tokizaki, and A. Nakamura, J. Phys. Condens. Matter **6**, 4581 (1994).
[30] S. Iwai, T. Tokizaki, A. Nakamura, K. Tanimura, N. Itoh, and A. Shluger, Phys. Rev. Lett. **76**, 1691 (1996).
[31] T. Shibata, S. Iwai, T. Tokizaki, K. Tanimura, A. Nakamura, and N. Itoh, Phys. Rev. B **49**, 13 255 (1994).
[32] C. J. Delbecq, W. Hayes, and P. H. Yuster, Phys. Rev. **121**, 1043 (1961).
[33] Y. Kondoh, M. Hirai, and M. Ueta, J. Phys. Soc. Jpn. **33**, 151 (1972).
[34] M. N. Kabler, in *Point Defects in Solids*, edited by J. H. Crawford, Jr. and L. M. Slifkin (Plenum, New York, 1972), p. 327.
[35] A. L. Shluger, V. E. Puchin, T. Suzuki, K. Tanimura, and N. Itoh, Phys. Rev. B **52**, 4017 (1995).
[36] The comparison between the temporal evolution of the *B* band in KBr:NO_2^- and that of the *F* band in pure KBr should be made using the data measured at the same temperature. However, it may be presumed that the formation time of the V_K center, and hence the decay time of the *B* band, at 273 K gives the shortest bound for the time at 80 K, since it is unlikely that the formation time of the V_K center is *delayed* at higher temperatures than at low temperatures. Therefore, the argument described here is considered to be reasonable.
[37] D. L. Dexter, C. C. Klick, and G. A. Russell, Phys. Rev. **100**, 603 (1955).
[38] A. Fukuda, S. Makishima, T. Mabuchi, and R. Onaka, J. Phys. Chem. Solids **28**, 1763 (1967).
[39] R. H. Bartram and A. M. Stoneham, Solid State Commun. **17**, 1593 (1975); A. M. Stoneham and R. H. Bartram, Solid State Electron. **21**, 325 (1978); R. H. Bartram and A. M. Stoneham, Semicond. Insul. **5**, 297 (1983).
[40] Y. Kayanuma and K. Nasu, Solid State Commun. **27**, 1371 (1978); K. Nasu and Y. Kayanuma, J. Phys. Soc. Jpn. **45**, 1341 (1978).
[41] M. C. M. O'Brien, J. Phys. C **5**, 2045 (1972).
[42] C. H. Leung and K. S. Song, Phys. Rev. B **18**, 922 (1978).
[43] T. Matsumoto, M. Shirai, and K. Kan'no, J. Phys. Soc. Jpn. **64**, 291 (1995).
[44] R. C. Baetzold and K. S. Song, J. Phys. Condens. Matter **3**, 2499 (1991).
[45] A. L. Shluger, R. W. Grims, and C. R. A. Catlow, J. Phys. Condens. Matter **3**, 3125 (1991).
[46] A. L. Shluger, N. Itoh, V. E. Puchin, and E. N. Heifets, Phys. Rev. B **44**, 1499 (1991).
[47] V. E. Puchin, A. L. Shluger, K. Tanimura, and N. Itoh, Phys. Rev. B **47**, 6226 (1993).
[48] V. E. Puchin, A. L. Shluger, and N. Itoh, Phys. Rev. B **52**, 6254 (1995).